Effect of Tetraacid on the Properties of ODPA/4,4′-ODA Polyimide Foams

Xiao-Yan Liu, Mao-Sheng Zhan, Yan-Xia Shen, Kai Wang

School of Materials Science and Engineering, Beijing University of Aeronautics and Astronautics, Beijing 100191, China

Received 28 January 2010; accepted 29 May 2010
DOI 10.1002/app.32899
Published online 27 September 2010 in Wiley Online Library (wileyonlinelibrary.com)

ABSTRACT: In this research, a new flexible polyimide (PI) foams was successfully prepared and characterized based on precursor powder foaming. This foams were derived from 3,3′,4,4′-oxydiphethalic anhydride (ODPA), 3,3′,4,4′-oxydiphethalic tetraacid (ODPA-tetraacid), and 4,4′-oxydianiline (4,4′-ODA). With varying molar percentage of ODPA-tetraacid in (ODPA + ODPA-tetraacid), the changes of properties of PI precursor powders and PI foams were comparatively investigated. The foaming processes of PI foams were observed by a self-made visualization device. The decomposition products of precursor powders were analyzed by thermogravimetry-Fourier transform infrared spectroscopy (TG-FTIR). The crystallinity of precursor powders was investigated by wide-angle X-ray diffraction (WXRD). The chemical structure of PI precursor powders and foams was analyzed by FTIR. The thermal properties of PI foams were tested by the methods of dynamic mechanical analysis (DMA), and TG/differential thermogravimetry (DTG) analysis. The cell structure of PI foams was observed by a scanning electron microscopy. The rebound resilience of PI foams was studied by a self-made drop-ball instrument. With the increasing of ODPA-tetraacid, the inflation onset temperatures and inflation degrees of PI foams decreased from 210°C to 118°C and increased from 10 to 14.8 times, respectively. The crystallinity of PI precursor powders increased. The thermal stability of PI foams decreased. The cell structure of PI foams became more uniform and the rebound rates increased linearly. Besides, ODPA-tetraacid did not yield any negative effect on the complete imidization of the PI precursor powder by the FTIR spectra. © 2010 Wiley Periodicals, Inc. J Appl Polym Sci 119: 3253–3263, 2011

Key words: polyimides; foams; ODPA-tetraacid; FTIR; rebound resilience; thermal properties

INTRODUCTION

Aromatic polyimides (PIs), by virtue of their outstanding thermal resistance, mechanical resistance, chemical resistance, and insulation properties, have secured a permanent place in many special applications from aircraft, spacecraft, marine ships to weapon, and automotive areas.[1–4] Newer to the arena of PIs is the preparation of PI foams, which were first developed by Dupont since 1966.[5] As for PI foams, many researchers have been focused on the high-thermal stability, low-density and high-mechanical strength, high-sound absorption coefficient, low-dielectric coefficient, good resistance to fire, and so on.[6–11] However, there has been few studies on the processable characteristics of precursors and the flexibility of PI foams.

Currently, the preparation of poly(amic acid) precursors that are suitable for low-temperature foaming are of great interest due to the lower cost and the high security.[12] Moreover, PI foams with certain flexibility may have a wider range of applications than the rigid ones. Weiser et al. prepared a kind of PI foams by using aromatic dianhydride, aromatic tetraacid, and aromatic diamine.[13,14] In his study, the densities, compression strength, limiting oxygen index, and glass transition temperature, expandability of PI foams were investigated. The effect of tetraacid on the properties of PI precursor powders and PI foams were neglected. In this article, the preparation and characterization of PI foams derived from 3,3′,4,4′-oxydiphethalic anhydride (ODPA), 3,3′,4,4′-oxydiphethalic tetraacid (ODPA-tetraacid), and 4,4′-oxydianiline (4,4′-ODA) will be presented. It is important to emphasize that the comparing properties of poly(amic acids) and PI foams in terms of varying molar percentage of ODPA-tetraacid in (ODPA + ODPA-tetraacid).

EXPERIMENTAL

Materials

The ODPA was purchased from Shanghai Research Institute of Synthetic Resins, China. 4,4′-ODA was obtained from Bengbu Zuguang Finechem Co., China. ODPA-tetraacid was self-made by hydrolyzing ODPA. Tetrahydrofuran (THF) and methanol were supplied by Beijing Finechem and used as

Correspondence to: M. Zhan (zhanms@buaa.edu.cn).

TABLE I
Compositions and Properties of PI Precursors and PI Foams

Molar percentage of ODPA-tetraacid in (ODPA + ODPA-tetraacid)/%	0	10	25	35	50
Precursor no.	PAA0	PAA10	PAA25	PAA35	PAA50
PIF no.	PIF0	PIF10	PIF25	PIF35	PIF50
Apparent viscosity (mPa s) (precursor solutions)	–[a]	1884	158	50	30
Density (kg m^{-3})	39. 96	40.03	40.01	39.89	39.04

[a] The apparent viscosity of PAA0 solution exceeded the range of test by the measurement.

blowing agent and the solvent. All dianhydride and tetraacid were dried in a vacuum oven for 8–10 h before use.

Preparation of poly(amic acids) and PI foams

The ODPA, ODPA-tetraacid, and 4,4′-ODA were weighed in an equimolar fashion, and THF and methanol were gauged according to a solid content of 20 wt %. Then, 4,4′-ODA was dispersed in a mixture of THF and methanol in a three-neck flask equipped with a mechanical stirrer at room temperature. To the stirring 4,4′-ODA solution, ODPA was added gradually with stirring in batches and the mixture was stirred for 8–12 h to yield a homogenous precursor solution. To this solution, ODPA-tetraacid was added gradually after ODPA dissolved completely.[13–15] Then the mixture was stirred for 6–8 h more at 30°C to yield a homogenous precursor solution. To ensure the number of amine groups equals the number of anhydride groups, the total molar amounts of ODPA plus ODPA-tetraacid should equal the molar amounts of 4,4′-ODA. In other words, the monomer molar ratio of 4,4′-ODA/(ODPA + ODPA-tetraacid) is 1.0.

The resulting poly(amic acid) solutions were then charged into stainless steel vats and treated in a vacuum oven at 60–70°C for 8 h. Then the materials were cooled and crushed into fine powders and separated by a sieve. The average particle size was determined by sieving the powders. The precursor powders were then treated for an additional amount of time (0–300 min) at 70°C to further reduce the residual solvents. Residual amounts of THF were determined by measuring proton nuclear magnetic resonance (NMR) spectra of the powders. The precursor fine powders were placed into molds. The molds were put into an oven at high temperature to obtain PI foams. As shown in Table I, various PI precursors and foams were obtained by changing ODPA-tetraacid content. The reaction equation and chemical structures of PI foams were shown in Figure 1. The possible reactions of salt-like structure in poly(amic acid) solutions were shown in Figure 2.[16,17]

Measurements

The apparent viscosity of poly(amic acid) solutions were measured by a NDJ-1 rotation viscometer. The foaming processes of PI foams were observed by a self-made visualization device at a heating rate of 10°C/min. In the self-made visualization device, the morphological change was observed by the Gui-Guang GL-99T stereo-microscope. A JVC digital color video camera and DH-CG300 video-capture card were used to capture and record the inflation morphologies. Wide-angle X-ray diffraction (WXRD) patterns of PI precursor powders were recorded by D/max2200 PC automatic X-ray diffractometer. Thermogravimetry-Fourier transform infrared spectroscopy (TG-FTIR) studies were ramped from 25°C to 800°C at a heating rate of 10°C/min under nitrogen atmosphere. FTIR performed with Nexus-470 to characterize the chemical structures and imidization degrees of PI precursor powders and PI foams. The Rheometric Scientific, dynamic mechanical analysis (DMA)-IV was used to carry out dynamic compressive mechanical analysis at a frequency of 1 Hz and a heating rate of 5°C/min in nitrogen from room temperature to 400°C. TGA was carried out with NETZSCH STA TGA-409C at a heating rate of 20°C/min from room temperature to 700°C under nitrogen atmosphere. The cell morphologies of PI foams were observed using a JSM-5800 scanning electron microscopy (SEM). The rebound resilience values of PI foams were tested according to ASTM D3574-81 by a self-made drop-ball instrument.

RESULTS AND DISCUSSION

Effect of ODPA-tetraacid content on the inflation onset temperatures and the inflation degree (θ) of PI precursor powders

In this section, the effect of ODPA-tetraacid content on the inflation onset temperatures, the inflation degree (θ) and the morphological changes of PI precursor powders during the foaming processes were investigated.[7,15,18–20] The particles with similar dimensions and microspheres with similar inflation shapes were surveyed to avoid the effect of initial particle dimension and inflation shape on the results. The inflation onset temperature was defined as the temperature at which the powders began to inflate [Fig. 4 (a)]. The inflation degree (θ) was indicated as V/V_0, where V was the average volume of initial particle. The particle volume (V) was defined

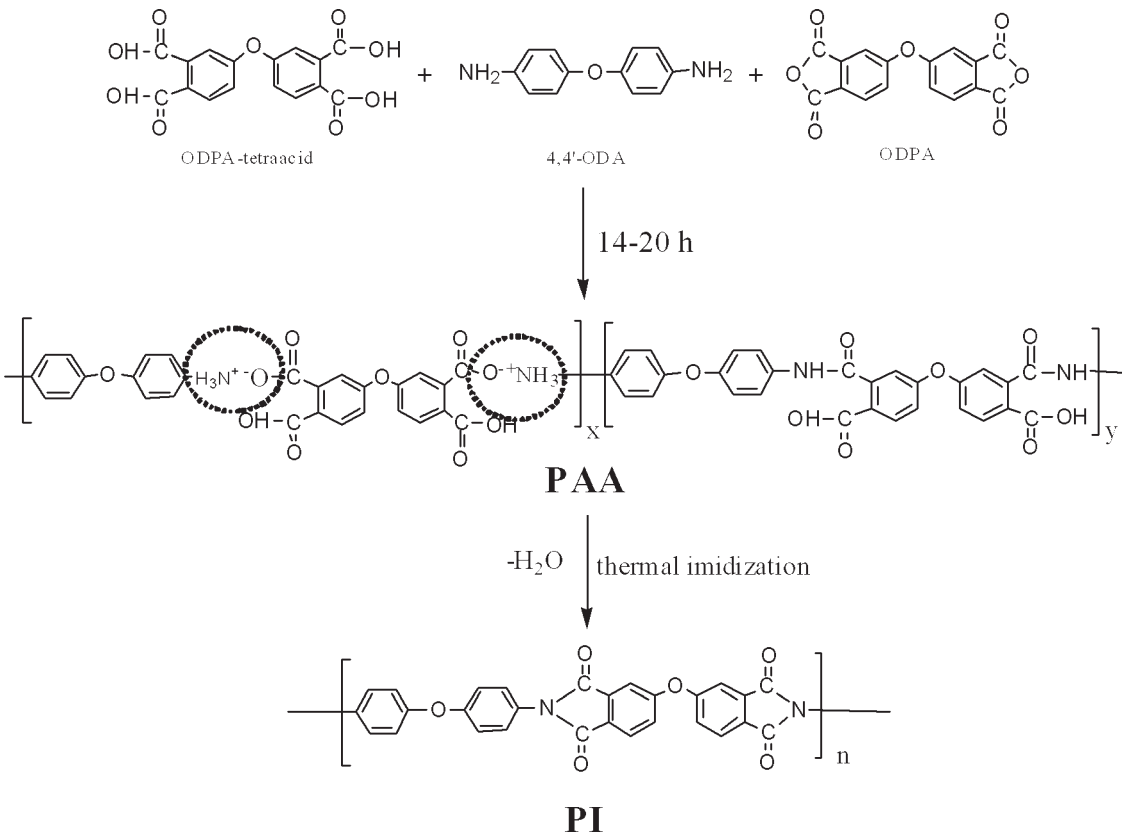

Figure 1 The reaction equation and chemical structure of poly(amic acid) and PI (x and y varied with the change of ODPA-tetraacid content).

as $\frac{4}{3}\pi(\frac{d}{2})^3$. The particle diameter (d) was defined as $(L_{max} + T_{max})/2$, where L_{max} was the maximum dimension of bubble and T_{max} was the maximum dimension in the direction perpendicular to the direction of L_{max} (Fig. 3).

The inflation onset temperatures and the inflation degree of PI precursor powders with temperature increasing at 10°C/min were shown in Figure 4(a). The temperatures of maximum foaming rate and foaming range versus ODPA-tetraacid molar percentage were shown in Figure 4(b). As shown in Figure 4(a), when temperature reached the inflation onset value, the volumes of all PI precursor powders expanded continuously to maximum values and then retained them despite of the continuous increase of temperature from room temperature to 350°C. The inflation onset temperatures of PAA0, PAA10, PAA25, PAA35, and PAA50 precursor

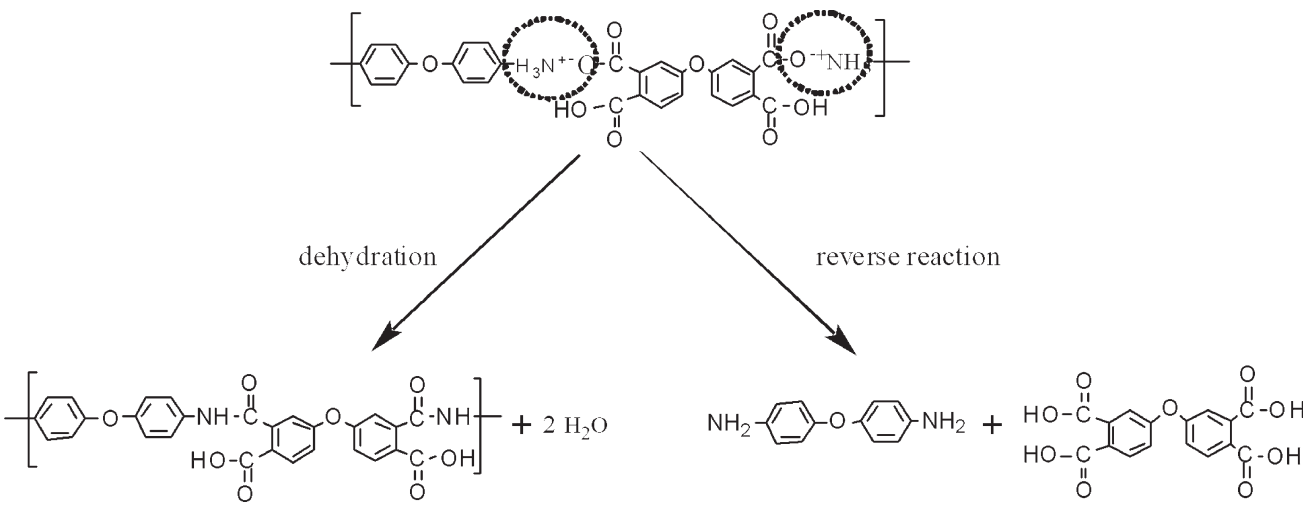

Figure 2 The possible reactions of salt-like structure in poly(amic acid) solutions.

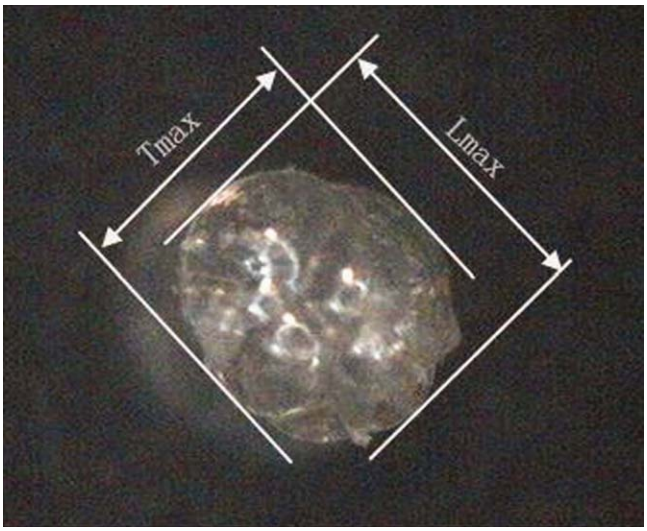

Figure 3 Scheme of dimension definition. [Color figure can be viewed in the online issue, which is available at wileyonlinelibrary.com.]

powders were about 208°C, 172°C, 150°C, 135°C, and 119°C, respectively. The inflation degree (θ) increased sequentially with the increase of ODPA-tetraacid.

This phenomena may result from the decreasing molecular weight of poly(amic acids) with the increase of ODPA-tetraacid. As shown in Table I, under the same conditions, the reduction in apparent viscosity of poly(amic acid) solutions with ODPA-tetraacid increased made it clearly that the molecular weight of poly(amic acids) were influenced. When ODPA-tetraacid mixed with 4,4′-ODA, a salt-like structure (—$O^{-}{}^{+}NH_3$—)might be synthesized and also dissociated partly (Figs. 1 and 2). This can cause a detrimental effect on the growth of molecular chains.[16] Besides, water generated from the reaction can certainly reverse the response direction and lower the equilibrium constant value. Thus, the molecular weight and apparent viscosity of poly(amic acids) decreased as ODPA-tetraacid increased. As illustrated in Figure 4(a), when temperature reached to a certain value, the volume of PAA50 powders with the highest ODPA-tetraacid content and the lowest molecular weight inflated first and continuous to a maximum value. The volume of PAA0 powders inflated at the highest temperature lastly. The temperatures of maximum foaming rate moved toward low temperature with increasing ODPA-tetraacid. The temperatures of foaming range changed a little [Fig. 4(b)].

The inflation degree of PI precursor powders increased with increasing of ODPA-tetraacid. It might be due to the varying content of volatile species. During the foaming processes, the residual solvents and water were the main volatile species contributing to the inflation of powders. The proportion of salt-like structure and carboxyl groups in poly(amic acid) was larger with higher ODPA-tetraacid content. When temperature rose, more water might be generated from the dehydration of salt-like structure and the reaction of carboxyl groups and amide groups. So the volatile species content and the inflation degree increased as ODPA-tetraacid increased. The morphological changes of PI precursor powders with increasing temperature were shown in Figure 5.

Analysis of TG-FTIR of PI precursor powders

TG curves of PAA0 and PAA50 powders at 10°C/min in nitrogen were shown in Figure 6. As shown in Figure 6, the TG curve of PAA0 moved toward high temperature. PAA0 and PAA50 powders had obvious weight losses before degradation when temperature reached up to 212°C and 121°C, respectively. There were two factors which caused the mass loss in the former step ranged from 120°C to 310°C: one was the volatilization of residual solvents, which is a physics process, and one

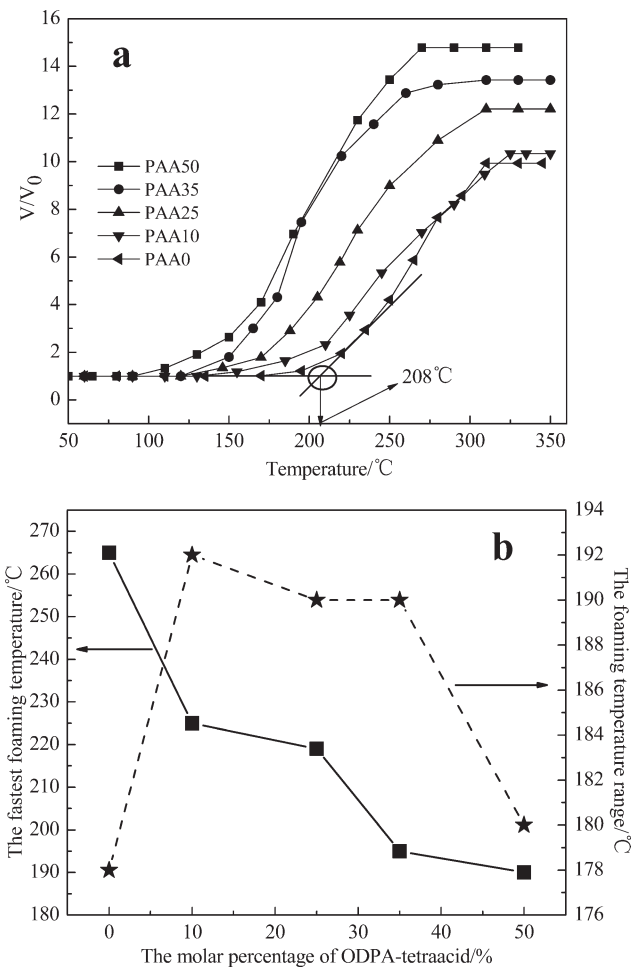

Figure 4 (a) The foaming process of PI precursor powders and (b) the temperatures of maximum foaming rate and foaming range of PI precursor powders.

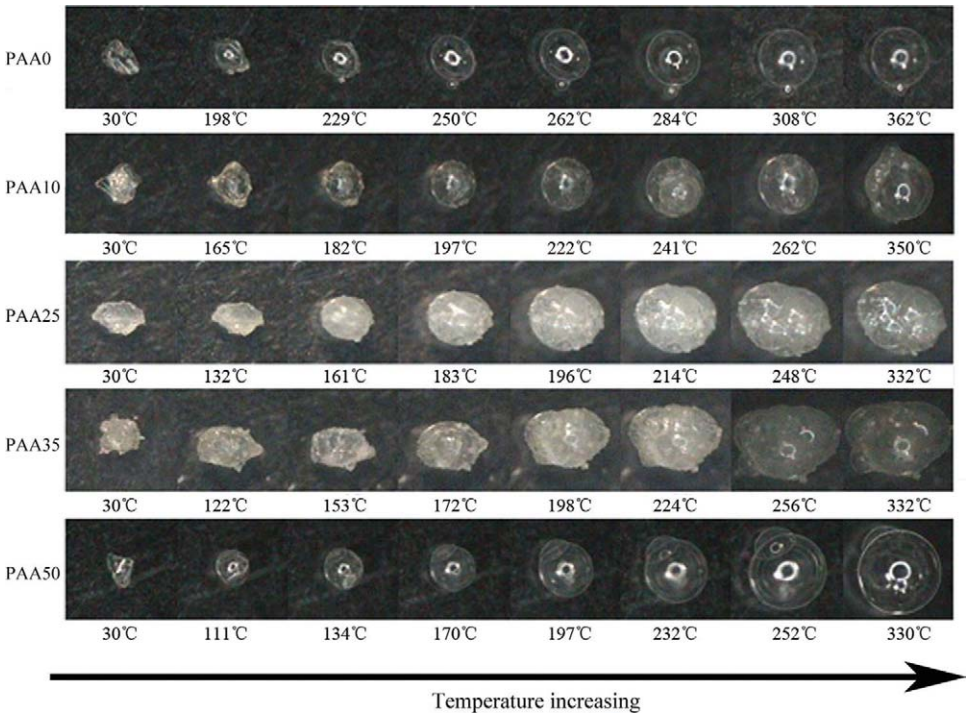

Figure 5 Morphological changes of PI precursor powders with increasing temperature. [Color figure can be viewed in the online issue, which is available atwileyonlinelibrary.com.]

reasonably supposed to be the cycloimidization of PAA to PI, which is a chemical process. As for the latter step, the mass loss primarily resulted from the pyrolysis of PI in high temperature. Powder foaming processes mainly depended on the volatile species and the small molecules generated during the cycloimidization in the former step essentially. The TG curves also revealed that the weight loss percentage of PAA50 was bigger than PAA0s.

Absorption strength of released gas (THF at 3002 cm^{-1}, H_2O at 3745 cm^{-1}, CO_2 at 2351 cm^{-1}, and CO at 2181 cm^{-1}) versus temperature in nitrogen of PAA0 and PAA50 powders were expressed in Figure 7.[21–24] The peak of THF mainly located in the temperature range of 102–200°C. The peaks of CO_2 and CO mainly located in the range of 485–800°C. The H_2O existed during the whole decomposition process, and part of them may absorbed from atmospheric moisture. The peaks of H_2O absorption were primarily around 130°C and 510°C. The intensities of H_2O absorption peaks for PAA50 were slight stronger than those for PAA0. It indicated that the decomposition H_2O was more in PAA50 than in PAA0.

Stacked plot of the FTIR spectra of by-products from the TG-FTIR during the degradation of PI precursor powders under the nitrogen environment were shown in Figure 8. It can be seen that the major gases evolved during the thermal degradation were THF, H_2O, CO_2, and CO. The characteristic peaks at 2780–3065 cm^{-1} and 919 cm^{-1} were assigned to stretching vibration of —CH_2— in THF. The stretching vibration of free O—H were in the range of 3500–3800 cm^{-1} and around 1600 cm^{-1}, which corresponded to the stretching vibration of H_2O. The characteristic bands of CO_2 were at 2350 cm^{-1} and 690 cm^{-1}. The characteristic band of CO was at 2180 cm^{-1}. As shown in Figure 8, the peaks of H_2O absorption of PAA50 powders were a little stronger than PAA0 powders. As for PAA50

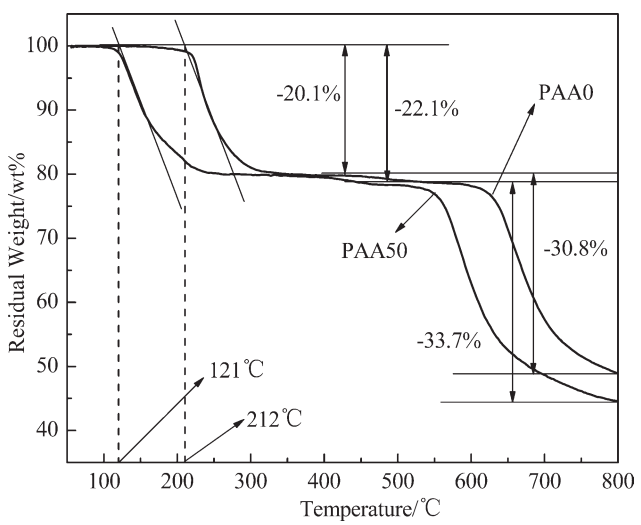

Figure 6 TG curves of PAA0 and PAA50 powders in nitrogen.

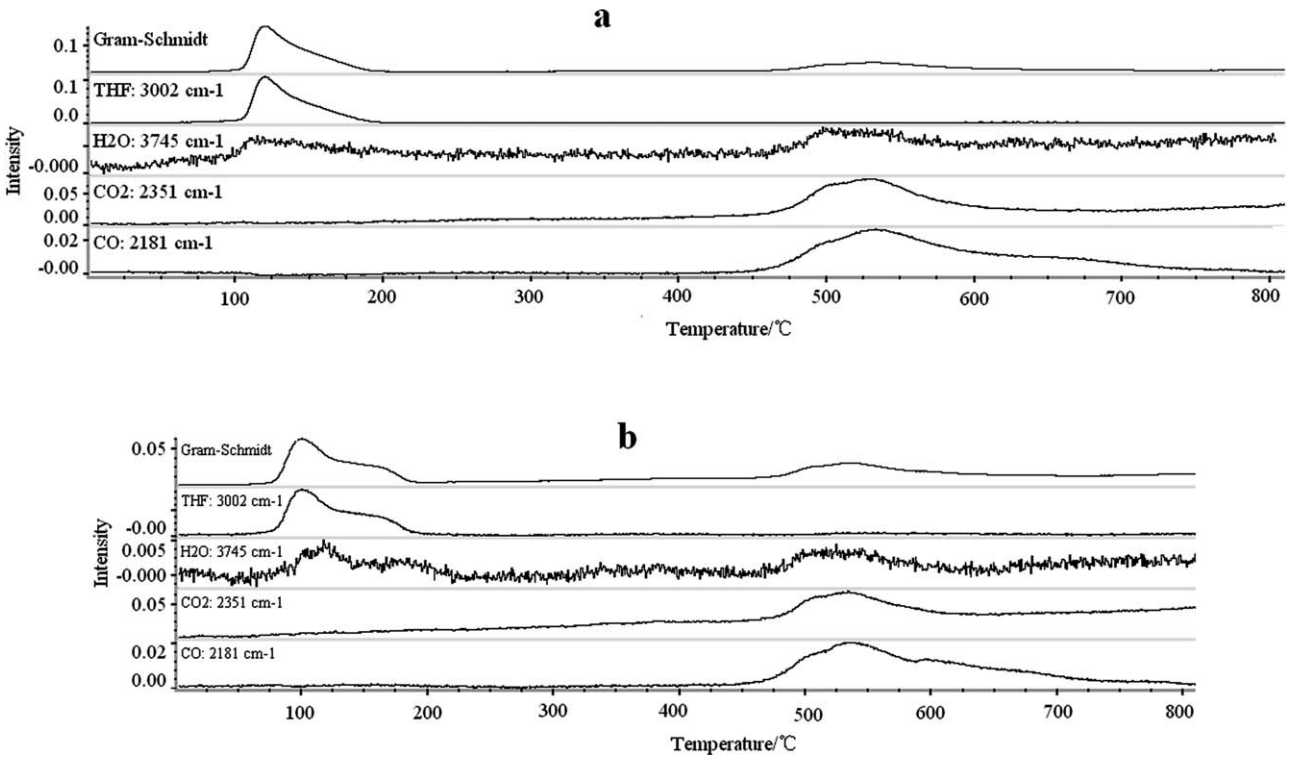

Figure 7 Absorption intensities for by-products measured by FTIR spectra with heating treatment temperature in nitrogen: (a) PAA0 powders and (b) PAA50 powders.

powders, the H_2O evolved at low temperature has been attributed to the dehydration of salt-like structure and the reaction of carboxyl groups and amide groups, and/or dehydration of unreacted ODPA-tetraacid end groups. With temperature increasing, the H_2O mainly result from the imidization and existed until the end of the decomposition process.

Analysis of WXRD of PI precursor powders

The crystallinity of PI precursor powders was characterized by WXRD in Figure 9. The X-ray diffraction curves of PAA0 and PAA10 powders expressed that they were basically amorphous. When the molar percentage of ODPA-tetraacid exceeded 25%, some wide peaks which suggested some degree of the short-range order in those powders were found. This might relate to the salt-like structure in the precursors and the relative flexible unit of ODPA-tetraacid. As we all know, salt tends to crystallize easily. When comparing with ODPA, increasing ODPA-tetraacid as a relative flexible unit can also increased the crystallinity of the products. Therefore, we can also infer that the salt-like structure might have been generated by the reaction of ODPA-tetraacid and 4,4′-ODA.

FTIR spectra of PI precursor powders and PI foams

The FTIR spectra of PI precursor powders and PI foams were illustrated in Figure 10(a,b), respectively. As shown in Figure 10(a), the FTIR spectra of PAA0 exhibited a slight sharp absorption band at about 3400 cm^{-1}, which corresponded to the absorption of —COOH and N—H. In comparison with the sample of PAA0, broad absorption bands appeared at 3000–3500 cm^{-1} indicated the existence of —COOH and N—H units for the other four PI precursor powders.[17,25–28] These might result from the absorption of carboxyl groups, which were ortho to the other carboxyl reacting with diamine. The other characteristic absorption peaks for the five PI precursor powders were similar. The absorption peaks at about 1716 cm^{-1} were assigned to the stretching vibration of C=O (—COOH). The peaks at about 1658 cm^{-1} were corresponded to the stretching vibration of C=O (—CONH). The peaks around 1550 cm^{-1} were representative of the existence of C—N bonds. The existence of the characteristic peaks suggested that PI precursor powders had the structure of —CONH—. Moreover, the peaks at 1500 cm^{-1} indicated the skeleton vibration of benzene ring. The characteristic absorption peaks located at about 2600 cm^{-1} confirmed the generation of ammonium salt-like structure.

In Figure 10(b), the infrared absorption spectrum curves of these PI foams generally resembled one another: the characteristic absorption peaks at 1777 cm^{-1} (asymmetrical C=O stretch) and 1721 cm^{-1} (symmetrical C=O stretch) indicated the existence of imide carbonyl. The peaks at 1380 cm^{-1} corresponded

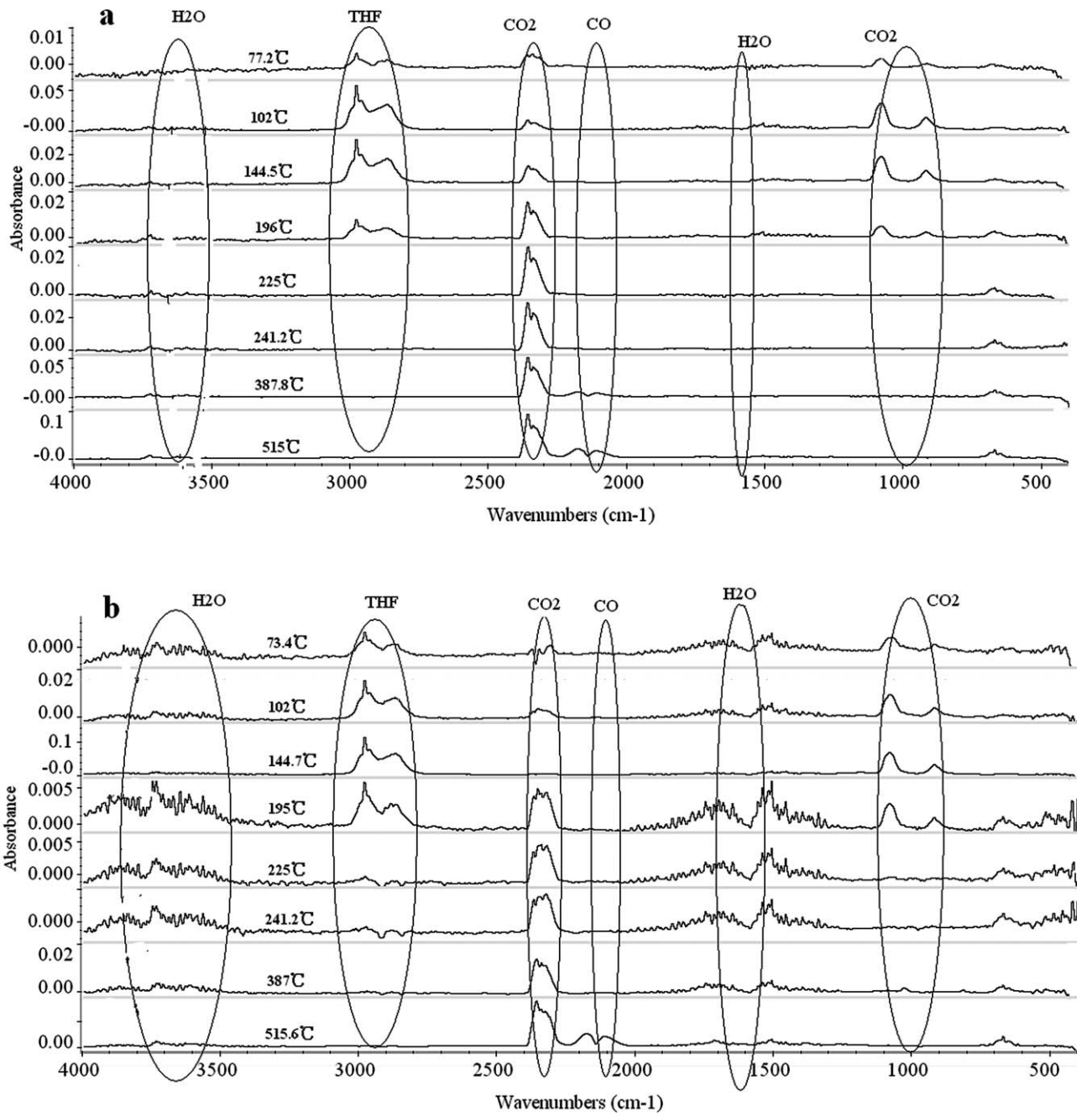

Figure 8 Stacked plot of the FTIR spectra of gases evolved from PI precursor powders in nitrogen: (a) PAA0 and (b) PAA50.

to the C—N stretching vibration of imide rings. The imide ring deformation vibration can be observed at 744 cm^{-1}. No amide carbonyl peaks at 1716 cm^{-1} or 1658 cm^{-1} were shown in the FTIR spectra. The characteristic absorption of —COOH end groups and N—H bond medium located in the region of 3000–3500 cm^{-1} disappeared thoroughly. This implied that the poly(amic acid) intermediates were completely converted into PIs. These results revealed that the adoption of ODPA-tetraacid did not have a negative effect on the imidization of PI precursor powders.

Thermal properties of PI foams

According to the previous contents, the inflation onset temperatures, the inflation degree, and the crystallinity of PI precursor powders were obviously influenced by the adoption of ODPA-tetraacid. The thermal properties of PI foams were evaluated by means of DMA and TGA, tabulated in Table II.[9,15,29] The T_g values and the maximum of loss tangent (tan δ) of PI foams were determined by DMA. As shown in Figure 11 and Table II, PIF0 exhibited the highest T_g value (~ 280°C), with PIF50 having the lowest T_g

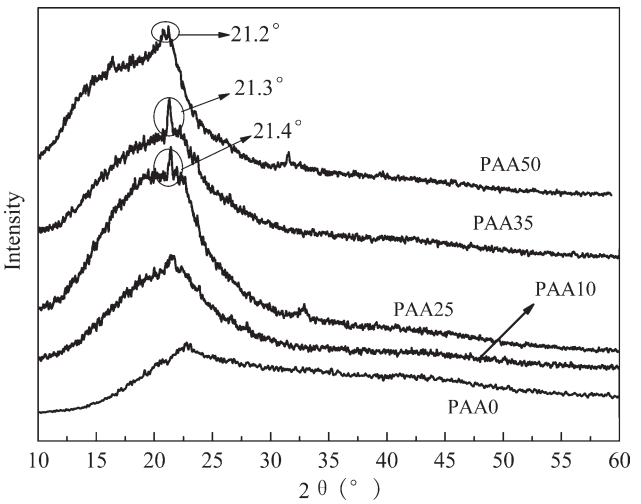

Figure 9 WXRD curves of PI precursor powders with varying ODPA-tetraacid content.

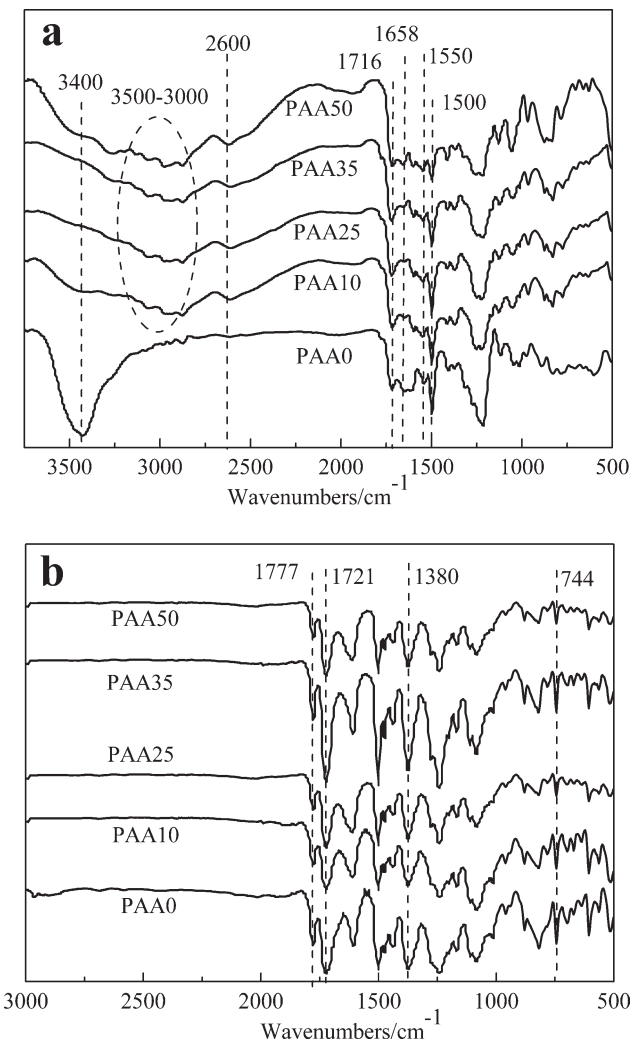

Figure 10 FTIR spectra: (a) PI precursor powders and (b) PI foams.

TABLE II
Thermal Properties of PI Foams

	Thermal properties					
PI foams	T_g(°C)	T_d(°C)	T_{max} (°C)	$T_{5\%}$ (°C)	$T_{10\%}$ (°C)	Char yield[a] (%)
PIF0	280	568.4	601.8	583.8	594.8	62.9
PIF10	274	561.6	597.1	579.2	591.5	59.2
PIF25	269	558.3	590.1	577.4	590.1	58.4
PIF35	265	551.8	585.8	573.6	587.8	58.2
PIF50	261	549.1	582.3	567.8	580.5	57.9

[a] Residual weight in TGA at 700°C under nitrogen atmosphere.

value of 261°C. When compared with PIF0, the ODPA-tetraacid-containing PI foams showed lower T_g values successively, but the values decreased slightly. The reduction of T_g values might be due to the relative low molecular weight and wide molecular weight distribution of the polymer chains, and the flexible unit of ODPA-tetraacid. The slight decrease of T_g values possibly related to the imidizaiton of PI precursor powders. During the conversion of poly(amic acid) to PI at high temperature, the carboxyl groups that were in the end of molecular chains or unreacted yet can transform into anhydride and still polymerize with amino. Also, the salt-like structure would convert to imide by cyclodehydration. When the imidization was accomplished completely, the molecular chains and the molecular weight of PI foams were affected slightly. These results were also confirmed by TG curves of PI foams showing in Figure 12.

What is more, the maximum values of tan δ shifted toward lower temperature region with the increase of ODPA-tetraacid. As the magnitude of tan δ increased significantly. These results indicated that PI foams with more ODPA-tetraacid would be easier to process. With ODPA-tetraacid increased, PI foams had lower molecular

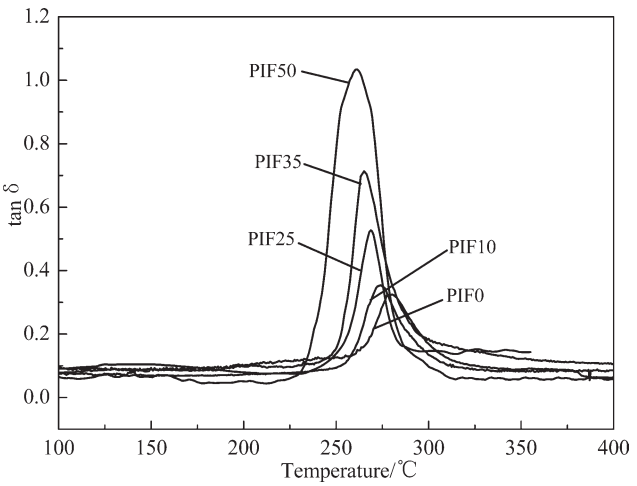

Figure 11 DMA curves of PI foams.

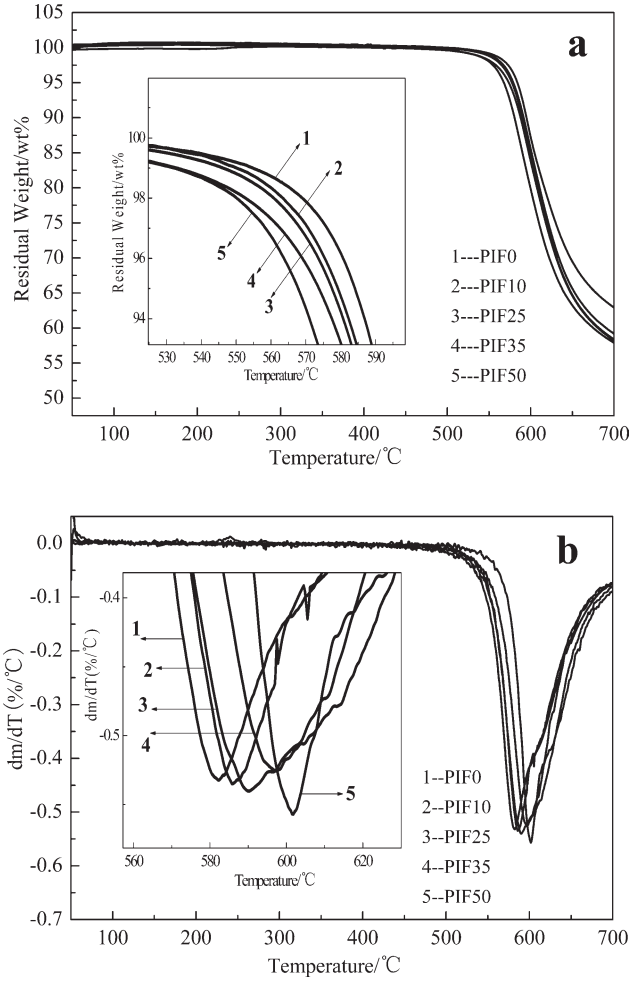

Figure 12 TG/DTG curves of PI foams: (a) TG curves and (b) DTG curves.

weight distribution, and high-excellent processability. The plasticity of the materials also increased with ODPA-tetraacid increasing.

TGA/DTG curves of PI foams were shown in Figure 12. The temperatures corresponding to the maximum decomposition occurring (T_{max}) of PI foams can be easily determined from DTG curves. The 5% weight loss temperatures ($T_{5\%}$), 10% weight loss temperatures ($T_{10\%}$), the decomposition-starting temperatures (T_d), T_{max} values, and the residual weight retentions (R_w) at 700°C of PI foams were given in Table II. PI foams did not experience any weight loss before the scanning temperature reached up to 540°C in nitrogen. As shown in Table II, the T_d values and T_{max} values of PI foams were in the range of 549–568°C and 582–602°C, respectively. The $T_{5\%}$ values and $T_{10\%}$ values were in the range of 567–583°C and 580–595°C, respectively. The experimental data implied that these PI foams possessed excellent thermal stability. In addition, the residual weight retentions at 700°C in nitrogen were all above 57%. Such high percentage of residual content at ~ 700°C also indicated the intrinsic fire-retardant property of these PI foams.

The results also expressed that the thermal stability of PI foams were slightly influenced by the adoption of ODPA-tetraacid. With the increase of ODPA-tetraacid, the thermal stability of PI foams decreased slightly. This was in agreement with the results of DMA test. Such stability was sufficient to meet the requirements of high-performance polymeric foam candidates for most potential applications.

Morphological observations of PI foams

The cross sectional SEM images of PI foams were displayed in Figure 13. Observed from the SEM images of these foams, the inner of samples showed that the cells of PI foams mainly existed in the form of closed pores, and the cell size in these foams ranged from 166 to 1000 μm. It was found that increasing ODPA-tetraacid can effectively improved the compactness and uniformity of the cell structure. As shown in Figure 13, the cell size of PI foams became smaller and more uniform as ODPA-tetraacid increased. The distribution of cell size became narrow. Large pores, small pores, and some broken pores can be observed in PIF0. All the pores in PIF0 were in a nonuniform distribution. It also can be found that PIF10, PIF25, PIF35, and PIF50 with uniform cell size had been successfully prepared. A more homogeneous size distribution of the cell size was obtained with the increase of ODPA-tetraacid. The cell walls of PIF35 and PIF50 were a little arised under the shooting of the electron gun. This phenomenon resulted from the flexibility of the molecular chains, on the one hand, and on the other hand, it also resulted from the increase of interaction of electrons and ionic bond of the salt-like structure in the molecular chains.

Rebound resilience of PI foams

According to the ASTM D3574-81, the rebound resilience of PI foams was tested by a self-made drop-ball instrument. The curve of rebound rates as a function of ODPA-tetraacid content was presented in Figure 14. As shown in Figure 14, with the increase of ODPA-tetraacid, the rebound rates of PI foams increased nearly in a straight line. The rebound rate of PIF50 was roughly 57% at the highest content of ODPA-tetraacid, whereas the rebound rates of PIF35, PIF35, and PIF10 were 51%, 48%, and 36%, respectively. The PIF0 showed a rebound rate minimum of ~ 30% with respect to no ODPA-tetraacid. The distinction might result from the flexibility of the molecular chains and the cell structure of PI foams. It can be inferred that the flexibility of the

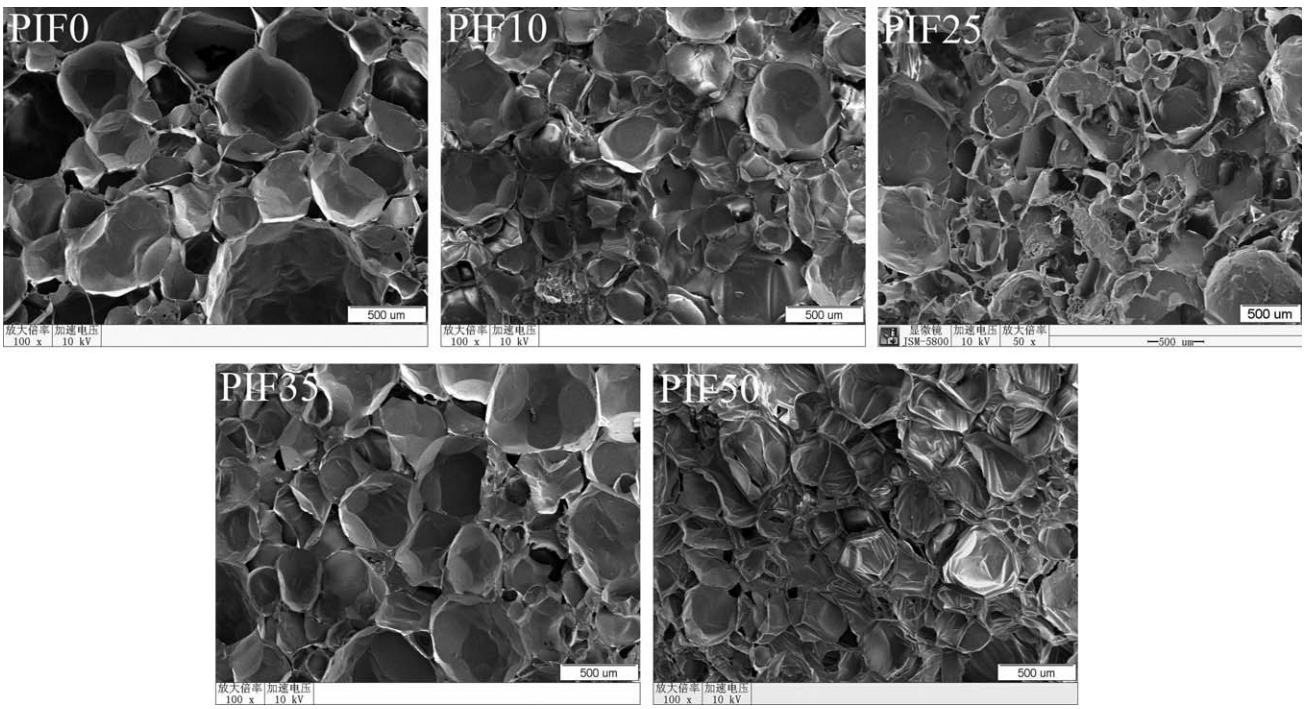

Figure 13 SEM images of PI foams.

matrix and the packing of cells of PI foams were influenced by the adoption of ODPA-tetraacid.

CONCLUSIONS

In this study, PI foams with low-process temperatures and high flexibility were successfully prepared. We have discussed the effects of ODPA-tetraacid on the properties of PI foams:

1. With the increase of ODPA-tetraacid, the apparent viscosity of poly(amic acid) solutions decreased obviously. The inflation onset temperatures of PI precursor powders decreased. The inflation degree is increased.
2. The weight loss percentage of PAA50 was bigger than PAA0s. The intensities of water absorption peaks for PAA50 were slight stronger than those for PAA0.
3. PI precursor powders showed a slight crystalline structure by WXRD when ODPA-tetraacid content exceeded 25%. The FTIR spectra indicated that ODPA-tetraacid had no negative effect on the imidization of PI precursor powders.
4. T_g values of PI foams were all above 260°C. The temperatures for 5 wt % mass loss were 567.8°C or higher, and 10 wt % mass loss were 580.5°C or greater. The temperatures for T_d were 549.1°C or higher, and T_{max} were 582.3°C or greater. The residual weight retentions at 700°C in nitrogen were all above 57%.
5. The SEM images of PI foams classified them as porous materials with uniform cell size by the adoption of ODPA-tetraacid. The rebound rates of PI foams increased significantly as the increase of ODPA-tetraacid. Consequently, the PI foams exhibited good flexibility.

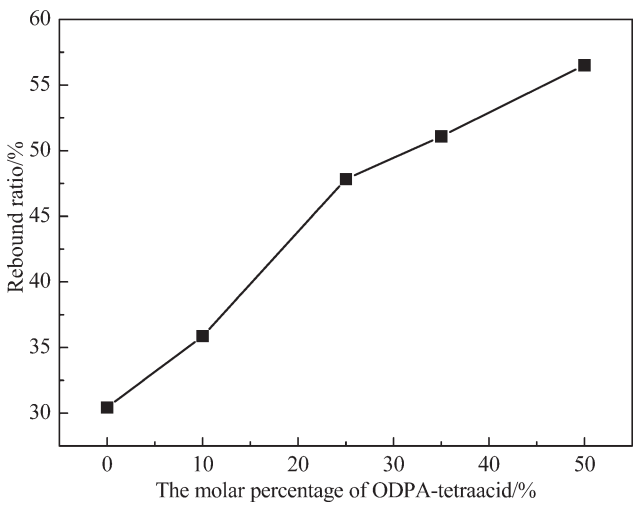

Figure 14 Resilient resilience curve of PI foams.

References

1. Kang, J. H.; Kim, Y. C.; Cho, K. J Appl Polym Sci 2006, 99, 3433.
2. Chung, C. M.; Lee, J. H.; Cho, S. Y.; Kim, J. G. J Appl Polym Sci 2006, 101, 532.
3. Zhao, X. J.; Liu, J. G.; Li, H. S.; Fan, L.; Yang, S. Y. J Appl Polym Sci 2009, 111, 2210.

4. Hedrick, J. L.; Charlier, Y.; Dipietro, R.; Jayaraman, S. J Polym Sci Part A: Polym Chem 1996, 34, 2867.
5. Hendrix, W. R.; Buffalo, N. Y.U.S. Pat. 3,249,561 (1966).
6. Hedrick, J. L.; Dipietro, R. Polymer 1996, 37, 5229.
7. Cano, C. I.; Weiser, E. S.; Kyu, T.; Byron Pipes, R. Polymer 2005, 46, 9296.
8. Weiser, E. S.; Johnson, T. F.; Clair, T. L. St.; Echigo, Y. High Perform Polym 2000, 12, 1.
9. Williams, M. K.; Holland, D. B.; Melendez, O.; Weiser, E. S. Polym Degrad Stab 2005, 88, 20.
10. Hshieh, F. Y.; Hirsch, D. B.; Beeson, H. D. Fire Mater 2003, 27, 119.
11. Caps, R.; Heinemann, U.; Fricke, J. Int J Heat Mass Transfer 1997, 40, 269.
12. Ding, M. X.; Polyimide—Materials and the Relationship of Chemical, Structure and Properties; Science Press, Beijing, 2006; Vol. 1, pp 6–7.
13. Weiser, E. S.; Clair, T. L. St.; Echigo, Y.; Kaneshiro, H.U.S. Pat. 6,133,330 (2000).
14. Weiser, E. S.; Clair, T. L. St.; Echigo, Y.; Kaneshiro, H.U.S. Pat. 6,180,746 (2001).
15. Shen, Y. X.; Zhan, M. S.; Wang, K. Polym Adv Technol, DOI: 10.1002/pat.1489, in press.
16. Ding, M. X.; Polyimide—Materials and the Relationship of Chemical, Structure and Properties; Beijing, 2006; Vol. 1, Chapter 2, pp 34–35.
17. Chu, H. J.; Zhu, B. K.; Xu, Y. Y. J Appl Polym Sci 2006, 102, 1734.
18. Pan, L. Y.; Shen, Y. X.; Zhan, M. S.; Wang, K. Polym Compos 2010, 31, 43.
19. Cano, C. I.; Clark, M. L.; Kyu, T.; Byron Pipes, R. Polym Eng Sci 2007, 47, 572.
20. Cano, C. I.; Kyu, T.; Byron Pipes, R. Polym Eng Sci 2007, 47, 560.
21. Shen, Y. X.; Zhan, M. S.; Wang, K.; Li, X. H. J Appl Polym Sci 2009, 115, 1680.
22. Chou, W. J.; Wang, C. C.; Chen, C. Y. Polym Degrad Stab 2008, 93, 745.
23. Meng, X. L.; Huang, Y. D.; Yu, H.; Lv, Z. S. Polym Degrad Stab 2007, 92, 962.
24. Zhao, S.; Shi, Z. Q.; Wang, C. Y.; Chen, M. M. J Appl Polym Sci 2008, 108, 1852.
25. Lu, Y. H.; Zhan, M. S. J Polym Sci Part A: Polym Phys 2005, 43, 2154.
26. Xu, Y. K.; Zhan, M. S.; Wang, K. J Polym Sci Part A: Polym Phys 2004, 42, 2490.
27. An, H. Y.; Zhan, M. S.; Wang, K. J Appl Polym Sci 2009, 114, 3987.
28. Li, Q.; Xu, Z. S.; Yi, C. F. J Appl Polym Sci 2008, 107, 797.
29. Williams, M. K.; Weiser, E. S.; Fesmire, J. E.; Grimsley, B. W. Polym Adv Technol 2005, 16, 167.